Local forest structure variability increases resilience to wildfire in dry western U.S. coniferous forests

Michael J. Koontz[1,2,3*], Malcolm P. North[2,4], Chhaya M. Werner[2,5,6], Stephen E. Fick[7,8], Andrew M. Latimer[2]

[1]Graduate Group in Ecology, University of California; Davis, CA, USA

[2]Department of Plant Sciences, University of California; Davis, CA, USA

[3]Earth Lab, University of Colorado-Boulder; Boulder, CO, USA

[4]Pacific Southwest Research Station, USDA Forest Service; Mammoth Lakes, CA, USA

[5]Center for Population Biology, University of California; Davis, CA, USA

[6]German Centre for Integrative Biodiversity Research; Halle-Jena-Leipzig, Germany

[7]US Geological Survey, Southwest Biological Science Center

[8]Department of Ecology and Evolutionary Biology, University of Colorado; Boulder, CO, USA

[*] *Correspondence:* 4001 Discovery Drive; Boulder, CO 80303; michael.koontz@colorado.edu; (970) 682-4727

Coauthor emails: mnorth@ucdavis.edu (MPN), cwerner@ucdavis.edu (CMW), stephen.fick@gmail.com (SEF), amlatimer@ucdavis.edu (AML)

Running title: Remote sensing resilience

Keywords: resilience, wildfire, severity, texture analysis, forest structure, Sierra Nevada, forest, disturbance

Type of article: Letters

Abstract word count: 149

Main text word count: 4805 (Intro: 930; Methods: 1631; Results: 558; Discussion: 1686)

Text boxes word count: 0

Number of... references: 106, figures: 5, tables: 1, text boxes: 0

Statement of authorship: MJK, CMW, SEF, MPN, and AML conceived the study. MJK, SEF, and CMW wrote the Earth Engine code. MJK performed the analysis, with input from all authors. MJK wrote the first draft of the manuscript. All authors contributed substantially to editing and revisions.

Data accessibility statement: The data and analysis code supporting the results are archived on the Open Science Framework at www.doi.org/10.17605/OSF.IO/27NSR.

Date report generated: August 27, 2019

Abstract

A "resilient" forest endures disturbance and is likely to persist. Resilience to wildfire may arise from feedback between fire behavior and forest structure in dry forest systems. Frequent fire creates fine-scale variability in forest structure, which may then interrupt fuel continuity and prevent future fires from killing overstory trees. Testing the generality and scale of this phenomenon is challenging for vast, long-lived forest ecosystems. We quantify forest structural variability and fire severity across >30 years and nearly 1,000 wildfires in California's Sierra Nevada. We find that greater variability in forest structure increases resilience by reducing rates of fire-induced tree mortality and that the scale of this effect is local, manifesting at the smallest spatial extent of forest structure tested (90m x 90m). Resilience of these forests is likely compromised by structural homogenization from a century of fire suppression, but could be restored with management that increases forest structural variability.

Introduction

Forests are essential components of the biosphere, and ensuring their persistence is of high management priority given their large carbon stores and other valued ecosystem services (1–4). Modern forests are subject to disturbances that are increasingly frequent, intense, and entangled with human society, which may compromise their resilience and their ability to persist (3, 5, 6). A resilient forest can absorb disturbances and may reorganize, but is unlikely to transition to an alternate vegetation type in the long run (7–10). Resilience can arise when interactions amongst heterogeneous elements within a system create stabilizing negative feedbacks, or interrupt positive feedbacks that would otherwise cause critical transitions (10, 11). System resilience can be generated by heterogeneity at a variety of organizational scales, including genetic diversity (12–14), species diversity (15–17), functional diversity (18), topoclimatic complexity (19, 20), and temporal environmental variation (21). Forest resilience mechanisms are fundamentally difficult to quantify because forests comprise long-lived species, span large geographic extents, and are affected by disturbances at a broad range of spatial scales (10, 22). It is therefore critical, but challenging, to understand the system-wide mechanisms underlying forest resilience and the extent to which humans have the capacity to influence them.

Wildfire severity describes a fire's effect on vegetation (23) and high-severity fire, in which all or nearly all overstory vegetation is killed, can be a precursor to state transitions in dry coniferous forests (24, 25). For several centuries prior to Euroamerican invasion, fire regimes in this ecosystem were variable, having primarily low- and moderate-severity fire, but localized patches of high-severity fire (26). Most dry coniferous tree species in frequent-fire forests did not evolve mechanisms to protect propagules (e.g., seeds, buds/stems that can resprout) through high-severity fire, so recruitment in large patches with few or no surviving trees is often highly limited by longer-distance dispersal of tree seeds from unburned or lower-severity areas (24, 27, 28). Absence of tree seeds after severe wildfire can lead to forest regeneration failure as resprouting shrubs outcompete slower-growing conifer seedlings and provide continuous cover of flammable fuel that makes future high-severity wildfire more likely (29, 30). Dry forest regeneration is especially imperiled after high-severity fire when post-fire climate conditions are suboptimal for conifer seedling establishment (25) or optimal for shrub regeneration (28).

Many dry western U.S. forests are experiencing "unhealthy" conditions which leaves them prone to catastrophic shifts in ecosystem type (3). First, warmer temperatures coupled with recurrent drought (i.e., "hotter droughts") exacerbate water stress on trees (3, 31, 32), producing conditions favorable for high-intensity fire (33, 34) and less suitable for post-fire conifer establishment (25, 35). Second, a century of fire suppression has drastically increased forest density and fuel connectivity (26), which favors modern wildfires with large, contiguous patches of tree mortality whose interiors are far from potential seed sources (24, 26, 36, 37). Thus, the presence of stabilizing feedbacks that limit high-severity fire may represent a fundamental resilience mechanism of dry coniferous forests, but anthropogenic climate and management impacts may be upsetting those feedbacks and eroding forest resilience.

An emerging paradigm in forest ecology is that resilience to disturbances such as wildfire may derive from heterogeneity in vegetation structure (38–40). Forest structure– the size and spatial distribution of vegetation in a forest– links past and future fire disturbance via feedbacks with fire behavior (41). A structurally variable forest with horizontally and vertically discontinuous fuel may experience slower-moving surface fires, a lower probability of crown fire initiation and spread, and a reduced potential for self-propagating, eruptive behavior (11, 42–45). Feeding back to influence forest structure, this milder fire behavior, characteristic of pre-Euroamerican settlement conditions in dry western U.S. forests, generates a heterogeneous patchwork of fire effects including consumed understory vegetation, occasional overstory tree mortality, and highly variable structure at a fine scale (26, 46, 47). Thus, more structurally variable dry forests are often considered more resilient and are predicted to persist in the face of frequent wildfire disturbance (38, 43, 48).

While the homogenizing effect of modern high-severity fire on forest structure is well-documented (37), the foundational concept of feedback between heterogeneity of forest structure and fire severity is underexplored, in part because of the challenge of measuring fine-scale heterogeneity at broad spatial extents (49). Furthermore, it has been difficult to empirically resolve the "scale of effect" (49) for how variability in forest structure is meaningful for resilience (50, 51).

Recent advances in the accessibility and tractability of spatiotemporally extensive Earth observation data (52) provide an avenue to insight into fundamental ecosystem properties at relevant scales, such as resilience mechanisms of vast, long-lived forests. We use Landsat satellite imagery and leverage a massively-parallel image processing approach to calculate wildfire severity for nearly 1,000 Sierra Nevada yellow pine/mixed-conifer wildfires encompassing a wide size range (4 to >100,000 hectares) and long time series (1984 to 2017). We calibrate these spectral severity measures to ground assessments of fire effects on overstory trees from over 200 field plots. For each point within these ~1,000 fires, we use texture analysis (53) at multiple scales in order to characterize local variability in vegetation structure across broad spatial extents and determine its "scale of effect" (49). We pair the resulting extensive database of wildfire severity and multiple scales of local forest variability to ask: (1) Does spatial variability in forest structure increase the resilience of California yellow pine/mixed-conifer forests by reducing the severity of wildfires? (2) What is the "scale of effect" of structural variability that influences wildfire severity? and (3) Does the influence of structural variability on fire severity depend on topography, regional climate, or other conditions?

Material and Methods

Study system

Our study assesses the effect of vegetation structure on wildfire severity in the Sierra Nevada mountain range of California in yellow pine/mixed-conifer forests (Fig. 1). This system is dominated by a mixture of conifer species including ponderosa pine (*Pinus ponderosa*), sugar pine (*Pinus lambertiana*), incense-cedar (*Calocedrus decurrens*), Douglas-fir (*Pseudotsuga menziesii*), white fir (*Abies concolor*), and red fir (*Abies magnifica*), angiosperm trees primarily including black oak (*Quercus kelloggii*), as well as shrubs (*Ceanothus* spp., *Arctostaphylos* spp.) (26). We considered "yellow pine/mixed-conifer forest" to be all areas designated as a yellow pine, dry mixed-conifer, or moist mixed-conifer pre-settlement fire regime (PFR) in the USFS Fire Return Interval Departure database (https://www.fs.usda.gov/detail/r5/landmanagement/gis/?cid=STELPRDB5327836), which reflects potential vegetation and is less sensitive to recent land cover change (37). We considered the Sierra Nevada region to be the area within the Sierra Nevada Foothills, the High Sierra Nevada, and the Tehachapi Mountain Area Jepson ecoregions (54).

A programmatic remote sensing assessment of wildfire severity

We measured forest vegetation characteristics and wildfire severity using imagery from the Landsat series of satellites (36, 55) post-processed to surface reflectance using radiometric corrections (56–59). Landsat

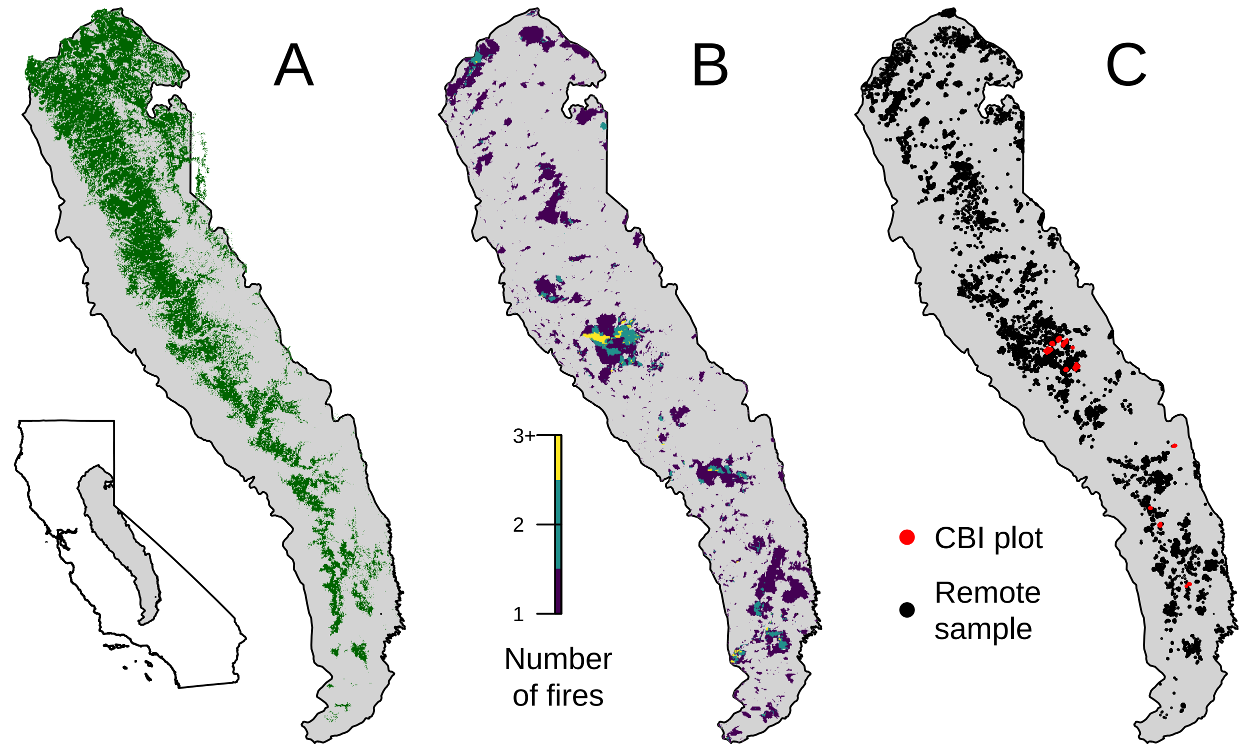

Fig. 1. Geographic setting of the study. A) Location of yellow pine/mixed-conifer forests as designated by the Fire Return Interval Departure (FRID) product which, among other things, describes the potential vegetation in an area based on the pre-Euroamerican settlement fire regime. B) Locations of all fires covering greater than 4 hectares that burned in yellow pine/mixed-conifer forest between 1984 and 2017 in the Sierra Nevada mountain range of California according to the State of California Fire Resource and Assessment Program database, the most comprehensive database of fire perimeters of its kind. Colors indicate how many fire perimeters overlapped a given pixel within the study time period. C) (red) Locations of 208 composite burn index (CBI) ground plots used to calibrate the remotely sensed measures of severity. (black) Locations of random samples drawn from 972 unique fires depicted in panel B that were in yellow pine/mixed-conifer forest as depicted in panel A, and which were designated as "burned" by exceeding a threshold relative burn ratio (RBR) determined by calibrating the algorithm presented in this study with ground-based CBI measurements.

satellites image the entire Earth approximately every 16 days with a 30m pixel resolution. We used Google Earth Engine, a massively parallel cloud-based geographic information system and image hosting platform, for all image collation and processing (52).

We calculated wildfire severity for the most comprehensive digital record of fire perimeters in California: The California Department of Forestry and Fire Protection, Fire and Resource Assessment Program (FRAP) fire perimeter database (http://frap.fire.ca.gov/projects/fire_data/fire_perimeters_index). Smaller fire events are important contributors to fire regimes, but their effects are often underrepresented in analyses of fire effects (60). The FRAP database includes all known fires that covered more than 4 hectares, compared to the regional standard database which includes fires covering greater than 80 hectares (36, 37, 61, 62) and the national standard Monitoring Trends in Burn Severity (MTBS) database which includes fires covering greater than 400 hectares in the western U.S. (55). Using the FRAP database of fire perimeters, we quantified fire severity within each perimeter of 972 wildfires in the Sierra Nevada yellow pine/mixed-conifer forest that burned between 1984 and 2017, which more than doubles the number of fire events represented from 430 to 972 compared to the regional standard database.

We created per-pixel median composites of collections of pre- and postfire images for each fire to calculate common spectral indices of wildfire severity. Prefire image collections spanned a fixed time window ending one day before the fire's discovery date and postfire image collections spanned the same fixed time window, exactly one year after the prefire window. We tested four different time periods (16, 32, 48, and 64 days) that defined the time window of the pre- and postfire image collections, and seven common spectral indices of severity (RBR, dNBR, RdNBR, dNBR2, RdNBR2, dNDVI, RdNDVI) for a total of 28 different means to remotely measure wildfire severity. See supplemental methods for full details of spectral measures of wildfire severity.

We calibrated these 28 severity metrics with 208 field measures of fire effects to overstory vegetation— the overstory component of the Composite Burn Index (CBI)— from two previously published studies (63, 64). CBI is a metric of vegetation mortality across several vertical vegetation strata within a 30m diameter field plot, and the overstory component characterizes fire effects to the overstory vegetation specifically (65). CBI ranges from 0 (no fire impacts) to 3 (very high fire impacts), and has a long and successful history of use as a standard for calibrating remotely-sensed severity data in western U.S. forests (36, 65–70). We interpolated each remotely-sensed severity metric using both bilinear (mean of 4 nearest pixels) and bicubic interpolation (mean of 16 nearest pixels) (67, 68, 70) and fit a non-linear model following (36), (66), (68), and (70) to each remotely-sensed severity metric of the following form:

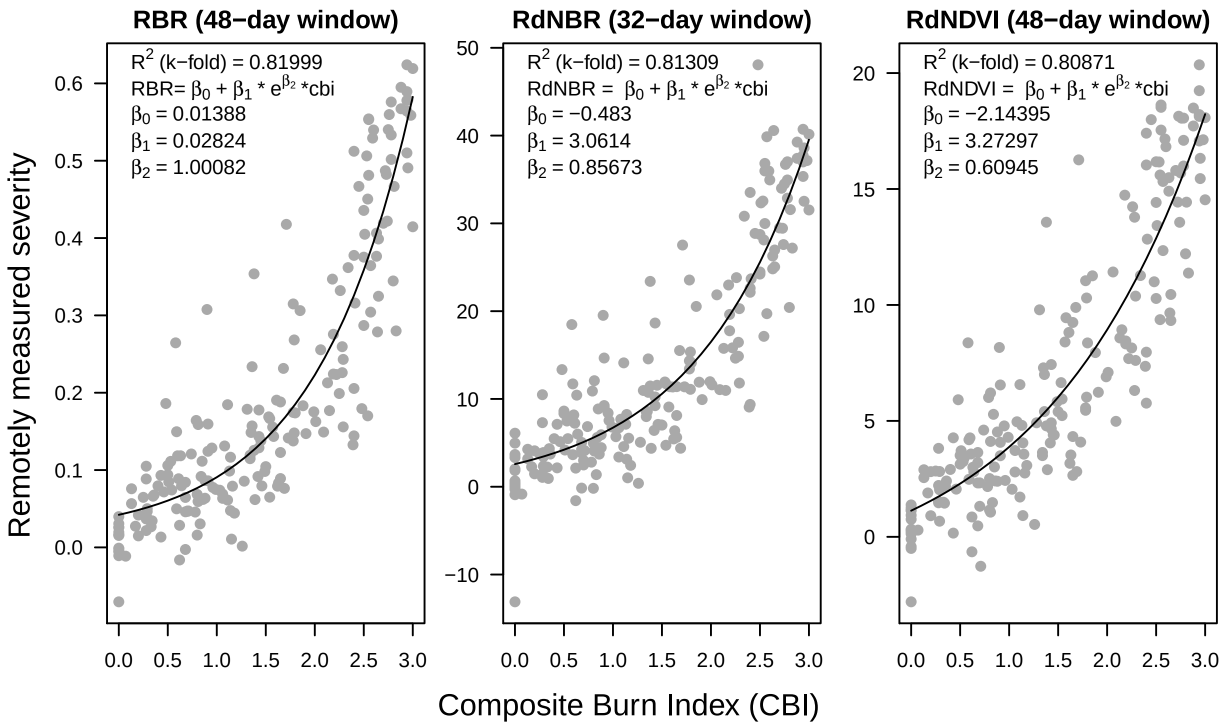

Fig. 2. Three top performing remotely-sensed severity metrics based on 5-fold cross validation (relative burn ratio, 48-day window, bicubic interpolation; relative delta normalized burn ratio, 32-day window, bilinear interpolation; and relative delta normalized difference vegetation index, 48-day window, bilinear interpolation) calculated using new automated image collation algorithms, calibrated to 208 field measures of fire severity (composite burn index). See Supplemental Table 1 for performance of all tested models.

(1) $\text{remote\_severity} = \beta_0 + \beta_1 e^{\beta_2 \text{cbi\_overstory}}$

We performed five-fold cross validation using the `modelr` and `purrr` packages in R (71–73). To compare goodness of model fits with (36), (66), and (68), we report the average R^2 value from the cross validation for each of the models. We used the severity calculation derived from the best fitting model from this comparison for all further analyses, which used a 48-day time window and the Relative Burn Ratio (RBR; (68)) spectral index (5-fold cross validation $R^2 = 0.82$; first panel of Fig. 2; Supp. Table 1). Example algorithm outputs are shown in Fig. 3.

Using the non-linear relationship between RBR and CBI from the best performing calibration model, we calculated the threshold RBR corresponding to “high-severity” signifying complete or near-complete overstory mortality using the common CBI high-severity lower threshold of 2.25 (i.e., an RBR value of 0.282) (36).

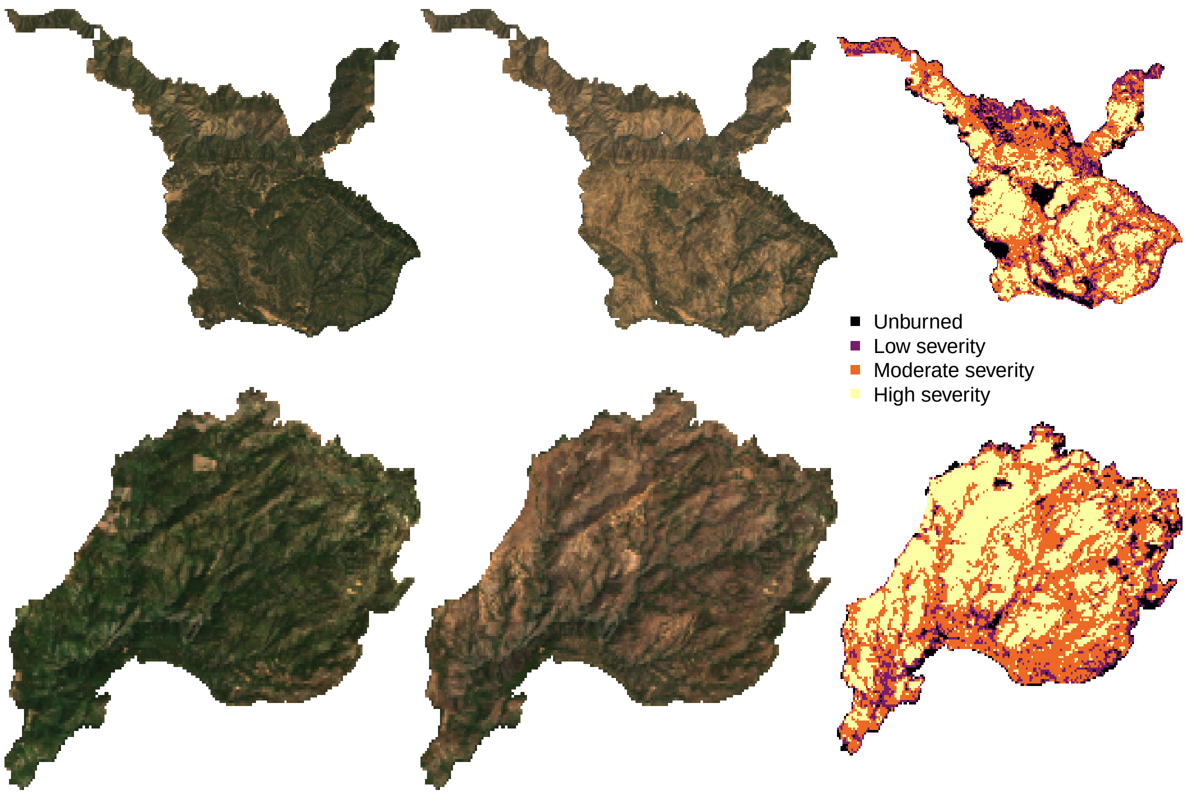

Fig. 3. Example algorithm outputs for the Hamm Fire of 1987 (top half) and the American Fire of 2013 (bottom half) showing: prefire true color image (left third), postfire true color image (center third), relative burn ratio (RBR) calculation using a 48-day image collation window before the fire and one year later (right third). For visualization purposes, these algorithm outputs have been resampled to a resolution of 100m x 100m from their original resolution of 30m x 30m. Data used for analyses were sampled from the outputs at the original resolution.

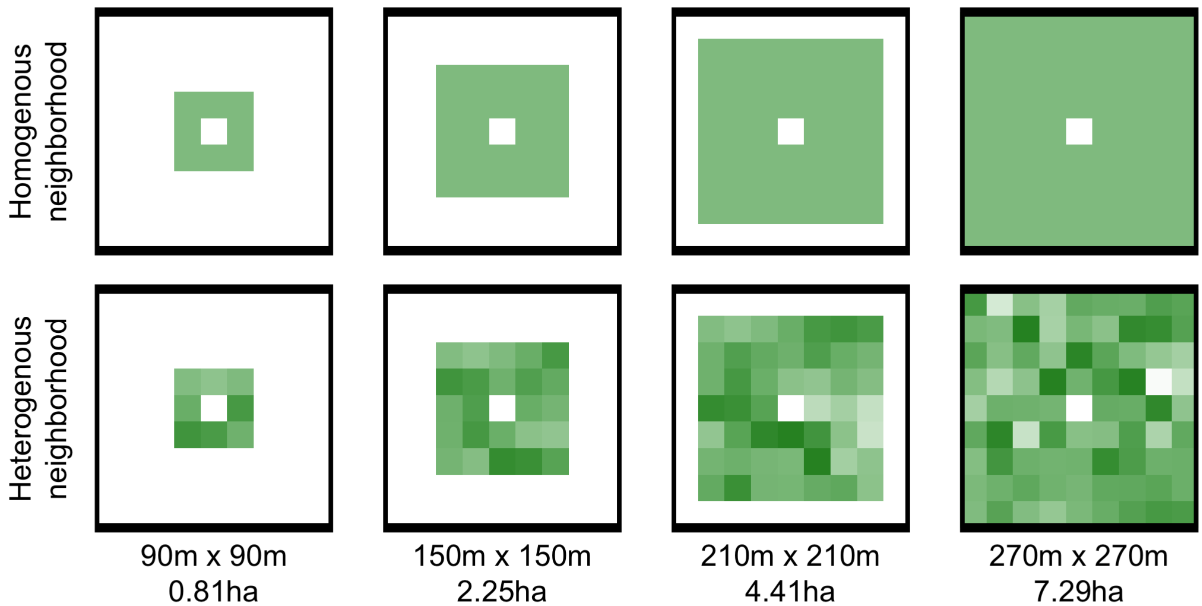

Fig. 4. Example of homogenous forest (top row) and heterogenous forest (bottom row) with the same mean NDVI values (~0.6). Each column represents forest structural variability measured using a different neighborhood size.

Remotely sensing local variability in forest structure at broad extents

We used texture analysis to calculate a remotely-sensed measure of local forest variability (53, 74). Within a moving square neighborhood window with sides of 90m (3x3 pixels), 150m (5x5 pixels), 210m (7x7 pixels), and 270m (9x9 pixels), we calculated forest variability for each pixel as the standard deviation of the NDVI values of its neighbors (not including itself). NDVI correlates well with foliar biomass, leaf area index, and vegetation cover (75), so a higher standard deviation of NDVI within a given local neighborhood corresponds to discontinuous canopy cover and abrupt vegetation edges (see Fig. 4) (76). Canopy cover is positively correlated with surface fuel loads including dead and down wood, grasses, and short shrubs (77, 78), which are primarily responsible for initiation and spread of "crowning" fire behavior which kills overstory trees (79).

Remote sensing other conditions

Topographic conditions

Elevation data were sourced from the Shuttle Radar Topography Mission (80), a 1-arc second digital elevation model. Slope and aspect were extracted from the digital elevation model. Per-pixel topographic roughness was calculated as the standard deviation of elevation values within the same-sized kernels as those used for variability in forest structure (90m, 150m, 210m, and 270m on a side and not including the central pixel).

We used the digital elevation model to calculate the potential annual heat load at each pixel, which is an integrated measure of latitude, slope, and a folding transformation of aspect about the northeast-southwest line ((81) with correction in (82); See Supplemental Methods for equations)

Moisture conditions

The modeled 100-hour fuel moisture data were sourced from the gridMET product, a gridded meteorological product with a daily temporal resolution and a 4km x 4km spatial resolution (83). We calculated 100-hour fuel moisture as the median 100-hour fuel moisture for the 3 days prior to the fire. The 100-hour fuel moisture is a correlate of the regional temperature and moisture which integrates the relative humidity, the length of day, and the amount of precipitation in the previous 24 hours. Thus, this measure is sensitive to multiple hot dry days across the 4km x 4km spatial extent of each grid cell, but not to diurnal variation in relative humidity nor to extreme weather events during a fire.

Remote samples

Approximately 100 random points were selected within each FRAP fire perimeter in areas designated as yellow pine/mixed-conifer forest and the values of wildfire severity as well as the values of each covariate were extracted at those points using nearest neighbor interpolation. Using the calibration equation described in Eq. 1 for the best configuration of the remote severity metric, we removed sampled points corresponding to “unburned” area prior to analysis (i.e., below an RBR threshold of 0.045). The random sampling amounted to 54109 total samples across 972 fires.

Modeling the effect of forest variability on severity

We used a hierarchical logistic regression model (Eq. 2) to assess the probability of high-severity wildfire as a linear combination of the remote metrics described above: prefire NDVI of each pixel, standard deviation of NDVI within a neighborhood (i.e., forest structural variability), the mean NDVI within a neighborhood, 100-hour fuel moisture, potential annual heat load, and topographic roughness. We included two-way interactions between the structural variability measure and prefire NDVI, neighborhood mean NDVI, and 100-hour fuel moisture. We include the two-way interaction between a pixel’s prefire NDVI and its neighborhood mean NDVI to account for structural variability that may arise from contrasts between these variables (e.g., “holes in the forest” vs. “isolated patches”; see Supplemental Fig. 2). We scaled all predictor variables, used weakly-regularizing priors, and estimated an intercept for each individual fire with pooled variance.

$$
\begin{aligned}
severity_{i,j} &\sim Bern(\phi_{i,j}) \\
(2) \quad logit(\phi_{i,j}) &= \beta_0 + \\
&\beta_{\mathrm{nbhd\_stdev\_NDVI}} * \mathrm{nbhd\_stdev\_NDVI}_i + \\
&\beta_{\mathrm{prefire\_NDVI}} * \mathrm{prefire\_NDVI}_i + \\
&\beta_{\mathrm{nbhd\_mean\_NDVI}} * \mathrm{nbhd\_mean\_NDVI}_i + \\
&\beta_{\mathrm{fm100}} * \mathrm{fm100}_i + \\
&\beta_{\mathrm{pahl}} * \mathrm{pahl}_i + \\
&\beta_{\mathrm{topographic\_roughness}} * \mathrm{topographic\_roughness}_i + \\
&\beta_{\mathrm{nbhd\_stdev\_NDVI*fm100}} * \mathrm{nbhd\_stdev\_NDVI}_i * \mathrm{fm100}_i + \\
&\beta_{\mathrm{nbhd\_stdev\_NDVI*prefire\_NDVI}} * \mathrm{nbhd\_stdev\_NDVI}_i * \mathrm{prefire\_NDVI}_i + \\
&\beta_{\mathrm{nbhd\_stdev\_NDVI*nbhd\_mean\_NDVI}} * \mathrm{nbhd\_stdev\_NDVI}_i * \mathrm{nbhd\_mean\_NDVI}_i + \\
&\beta_{\mathrm{nbhd\_mean\_NDVI*prefire\_NDVI}} * \mathrm{nbhd\_mean\_NDVI}_i * \mathrm{prefire\_NDVI}_i + \\
&\gamma_j \\
\gamma_j &\sim \mathcal{N}(0, \sigma_{\mathrm{fire}})
\end{aligned}
$$

Assessing the "scale of effect" of forest structure variability

Each neighborhood size (90m, 150m, 210m, 270m on a side) was substituted in turn for the neighborhood standard deviation of NDVI, neighborhood mean NDVI, and terrain ruggedness covariates to generate a candidate set of 4 models. To assess the scale at which the forest structure variability effect manifests, we compared the 4 candidate models based on different neighborhood sizes using leave-one-out cross validation (LOO cross validation) (84). We inferred that the neighborhood size window used in the best-performing model reflected the scale at which the forest structure variability effect had the most support (49).

Statistical software

We used `R` for all statistical analyses (73). We used the `brms` package to fit mixed effects models in a Bayesian framework which implements the No U-Turn Sampler (NUTS) extension to the Hamiltonian Monte Carlo algorithm (85, 86). We used 4 chains with 3000 samples per chain (1500 warmup samples and 1500 posterior samples) and chain convergence was assessed for each estimated parameter by ensuring Rhat values were less than or equal to 1.01 (86).

Data availability

All data and analysis code are available via the Open Science Framework (DOI: 10.17605/OSF.IO/27NSR) including a new dataset representing wildfire severity, vegetation characteristics, and regional climate conditions within the perimeters of 1,090 fires from the FRAP database that burned in yellow pine/mixed-conifer forest in the Sierra Nevada, California between 1984 and 2017.

Results

Programmatic assessment of severity

Our method to calculate remotely sensed severity using automated Landsat image fetching calibrates as well or better to ground-based severity data than most other reported methods that use hand-curation of Landsat imagery (see review in (87)). Further, several combinations of remotely sensed severity metrics, time windows, and interpolation methods validate well with the ground-based severity metrics, including those based on NDVI which is calculated using reflectance in shorter wavelengths than those typically used for measuring severity (Fig. 2). The top three configurations of our remotely sensed severity metric are depicted in Fig. 2.

Scale of effect of forest structure variability

Tab. 1: Comparison of four models described in Eq. 2 using different neighborhood sizes for calculating forest structural variability (standard deviation of NDVI within the neighborhood), neighborhood mean NDVI, and topographic roughness. LOO is a measure of a model's predictive accuracy (with lower values corresponding to more accurate prediction) and is calculated as -2 times the expected log pointwise predictive density (elpd) for a new dataset (84). ΔLOO is the difference between a model's LOO and the lowest LOO in a set of models (i.e., the model with the best predictive accuracy). The Bayesian R^2 is a 'data-based estimate of the proportion of variance explained for new data' (88). Note that Bayesian R^2 values are conditional on the model so shouldn't be compared across models, though they can be informative about a single model at a time.

Model	Neighborhood size for variability measure	LOO (-2*elpd)	Δ LOO to best model	SE of Δ LOO	LOO model weight (%)	Bayesian R^2
1	90m x 90m	40786	0	NA	100	0.299
2	150m x 150m	40842	56.03	14.69	0	0.298
3	210m x 210m	40883	96.87	20.94	0	0.297
4	270m x 270m	40912	125.9	24.73	0	0.297

The model with the best out-of-sample prediction accuracy assessed by leave-one-out cross validation was the model fit using the smallest neighborhood size for the variability of forest structure (standard deviation of neighborhood NDVI), the mean of neighborhood NDVI, and the terrain roughness (standard deviation of elevation) (Tab. 1). Model weighting based on the LOO score suggests 100% of the model weight belongs to the model using the smallest neighborhood size window.

Effects of prefire vegetation density, 100-hour fuel moisture, potential annual heat load, and topographic roughness on wildfire severity

We report the results from fitting the model described in Eq. 2 using the smallest neighborhood size (90m x 90m) because this was the best performing model (see above) and because the size and magnitude of estimated coefficients were similar across neighborhood sizes (See Supp. Table 2 for a summary of all parameter estimates for all models).

The strongest influence on the probability of a forested area burning at high-severity was the density of the vegetation, as measured by the prefire NDVI at that central pixel. A greater prefire NDVI led to a greater probability of high-severity fire ($\beta_{\text{prefire\_ndvi}} = 1.044$; 95% CI: [0.911, 1.174]); Fig. 5). There was a strong negative relationship between 100-hour fuel moisture and wildfire severity such that increasing 100-hour fuel moisture was associated with a reduction in the probability of a high-severity wildfire ($\beta_{\text{fm100}} = -0.569$; 95% CI: [-0.71, -0.423]) (Fig. 5). Potential annual heat load, which integrates aspect, slope, and latitude, also had a strong positive relationship with the probability of a high-severity fire. Areas that were located on southwest facing sloped terrain at lower latitudes had the highest potential annual heat load, and they were more likely to burn at high-severity ($\beta_{\text{pahl}} = 0.239$; 95% CI: [0.208, 0.271]) Fig. 5). We found a negative effect of the prefire neighborhood mean NDVI on the probability of a pixel burning at high-severity ($\beta_{\text{nbhd\_mean\_NDVI}} = -0.14$; 95% CI: [-0.278, 0.002]). This is in contrast to the positive effect of the prefire NDVI of the pixel itself. We found no effect of local topographic roughness on wildfire severity ($\beta_{\text{topographic\_roughness}} = -0.01$; 95% CI: [-0.042, 0.022]).

There was also a strong negative interaction between the neighborhood mean NDVI and the prefire NDVI of the central pixel ($\beta_{\text{nbhd\_mean\_NDVI*prefire\_NDVI}}$ -0.573; 95% CI: [-0.62, -0.526]).

Effect of variability of vegetation structure on wildfire severity

From the same model, we found strong evidence for a negative effect of variability of vegetation structure on the probability of a high-severity wildfire ($\beta_{\text{nbhd\_stdev\_NDVI}} = -0.208$; 95% CI: [-0.247, -0.17]); Fig. 5).

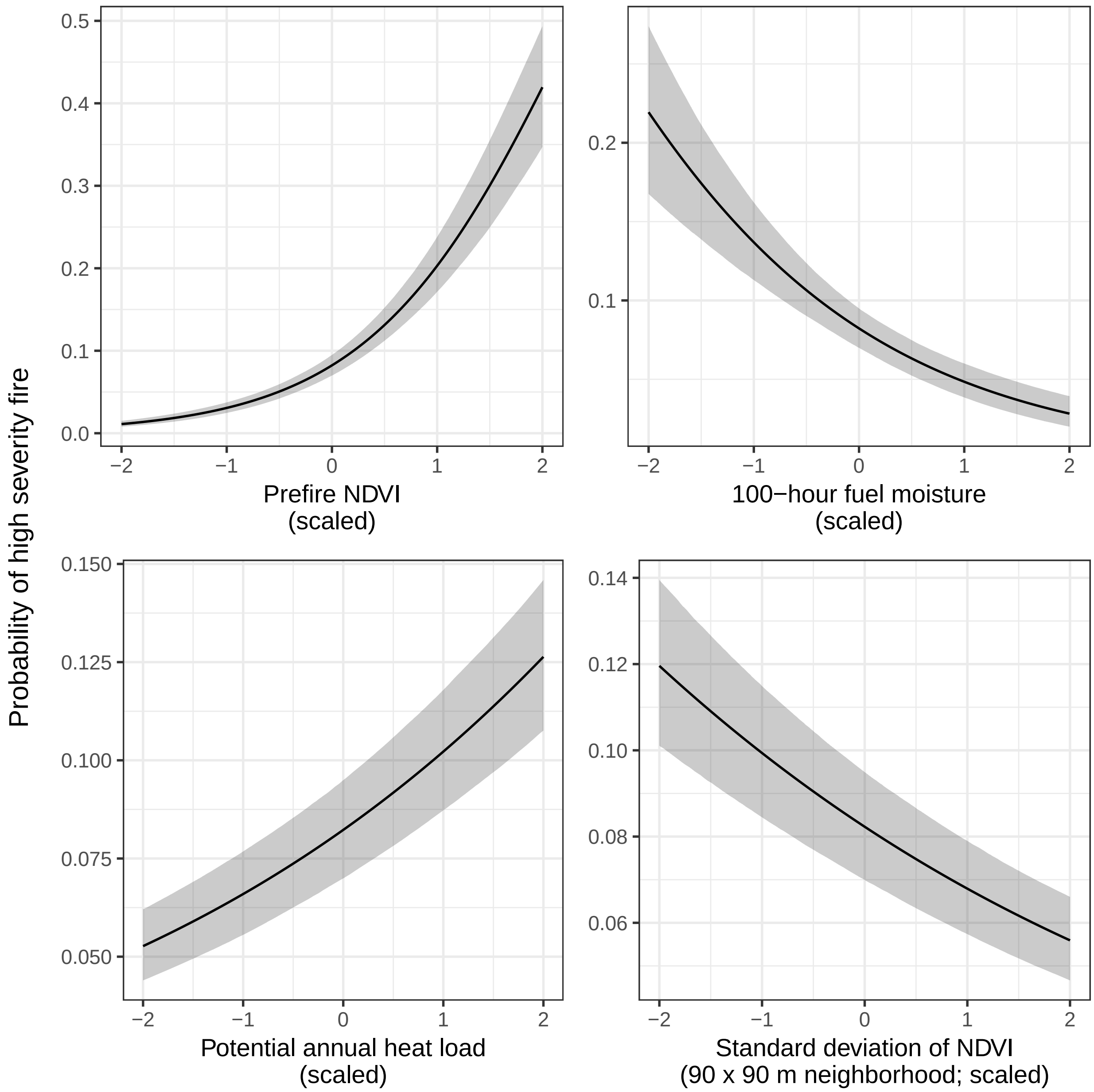

Fig. 5. The main effects and 95% credible intervals of the covariates having the strongest relationships with the probability of high-severity fire. All depicted relationships derive from the model using the 90m x 90m neighborhood size window for neighborhood standard deviation of NDVI, neighborhood mean of NDVI, and topographic roughness, as this was the best performing model of the four neighborhood sizes tested. The effect sizes of these covariates were similar for each neighborhood size tested.

We also found significant interactions between variability of vegetation structure and prefire NDVI of the central pixel $\beta_{\text{nbhd\_stdev\_NDVI*prefire\_NDVI}}$ = 0.125; 95% CI: [0.029, 0.218]) as well as between variability of vegetation structure and neighborhood mean NDVI ($\beta_{\text{nbhd\_stdev\_NDVI*nbhd\_mean\_NDVI}}$ = -0.129; 95% CI: [-0.223, -0.034]).

Discussion

Broad-extent, fine-grain, spatially-explicit analyses of whole ecosystems are key to illuminating macroecological phenomena such as forest resilience (89). We used a powerful, cloud-based geographic information system and data repository, Google Earth Engine, as a 'macroscope' (90) to study feedbacks between vegetation structure and wildfire disturbance in yellow pine/mixed-conifer forests of California's Sierra Nevada mountain range. With this approach, we reveal and quantify general features of this forest system, and gain deeper insights into the mechanisms underlying its function.

High-severity wildfire in the context of ecological resilience

Wildfire severity can be considered a direct correlate of a forest's resistance– the ease or difficulty with which a disturbance changes the system state (8, 91). One relevant state change for assessing ecosystem resistance is the loss of its characteristic native biota (92), which could be represented as overstory tree mortality (e.g., severity) in a forested system. The same fire behavior in two different forest systems (e.g., old-growth conifer versus young conifer plantation) may have very different abilities to cause overstory mortality (23), which reflects differences in each forest's resistance. Resistance is a key component of resilience (8, 91) and, in this framework, one manifestation of forest resilience is high resistance to wildfire, whereby some mechanism leads to lower severity when a fire occurs. Here, we show clear evidence that structural heterogeneity fulfills this mechanistic resistance role in dry coniferous systems (Fig. 5). This does not imply that resistance to fire is the only (or a necessary) path to resilience. For instance, high-severity fire is characteristic of other forest systems such as serotinous lodgepole pine forests in Yellowstone National Park, and is not ordinarily expected to hamper forest regeneration (93). Our inference that structural variability is a fundamental resilience mechanism in dry coniferous forests is strengthened by its large effect size and our ability to measure the negative feedback phenomenon at relevant spatiotemporal scales: we captured local-scale variability in structure and wildfire severity at broad spatial extents for an extensive set of nearly 1,000 fires across a 33-year time span.

Factors influencing the probability of high-severity wildfire

We found that the strongest influence on the probability of high-severity wildfire was prefire NDVI. Greater NDVI corresponds to high canopy cover and vegetation density (75) which translates directly to live fuel loads in the forest canopy and can increase high-severity fire (70). Overstory canopy cover and density also correlate with surface fuel loads (77, 78), which play a larger role in driving high-severity fire compared to canopy fuel loads in these forests (79). Thus NDVI is likely a strong predictor of fire severity because it is correlated with both surface fuel loads and canopy live fuel density.

We found a strong positive effect of potential annual heat load as well as a strong negative effect of 100-hour fuel moisture, results which corroborates similar studies (70). Some work has shown that terrain ruggedness (94), and particularly coarser-scale terrain ruggedness (95), is an important predictor of wildfire severity, but we found no effect using our measure of local terrain variability.

Critically, we found a strong negative effect of forest structural variability on wildfire severity that was opposite in direction but similar in magnitude to the effect of potential annual heat load. Just as the positive effect of NDVI is likely driven by surface fuel loads, the negative effect of variability in NDVI (our measure of structural variability), is likely driven by discontinuity in surface fuel loads, which can reduce the probability of initiation and spread of tree-killing crown fires (41, 43, 96, 97). The strong influence of a decreased connectivity of fuels at a local scale suggests that heterogeneity in forest structure may also influence broader-scale wildfire behavior and effects via cross-scale interactions (11, 98).

Feedback between forest structural variability and wildfire severity

This system-wide inverse relationship between structural variability and wildfire severity closes a feedback that links past and future fire behavior via forest structure. Frequent wildfire in dry coniferous forests generates variable forest structure (39, 99, 100), which in turn, as we demonstrate, dampens the severity of future fire. In contrast, exclusion of wildfire homogenizes forest structure and increases the probability that a fire, when it occurs, will produce large, contiguous patches of overstory mortality (24, 37). The proportion and spatial configuration of fire severity in fire-prone forests are key determinants of their long-term persistence (24, 37). Lower-severity fire or scattered patches of higher-severity fire reduce the risk of conversion to a non-forest vegetation type (24, 101), while prospects for forest regeneration are bleak when high-severity patch sizes are much larger than the natural range of variation for the system (3, 24, 26, 30, 44, 102, 103). Thus, the forest-structure-mediated feedback between past and future fire severity underlies the resilience of the Sierra Nevada yellow pine/mixed-conifer system.

Scale of effect of variability in forest structure

We found that the effect of a forest patch's neighborhood characteristics on the probability of high-severity fire was strongest at the smallest neighborhood size that we tested, 90m x 90m. This suggests that the moderating effect of variability in vegetation structure on fire severity is a very local phenomenon. This corroborates work by (104), who found that crown fires (with high tree killing potential) were almost always reduced to surface fires (with low tree killing potential) within 70m of entering an fuel reduction treatment area.

Severity patterns at a landscape scale (e.g., for a whole fire) may represent cross-scale emergences (89) of very local interactions between forest structure and fire behavior. For instance, forest management actions (e.g., prescribed fire, use of wildfire under mild conditions) that reduce fuel loads and increase structural variability can be effective at reducing fire severity across broader spatial extents than the direct footprints of those actions (43, 44, 105). Some work suggests that this sort of cross-scale emergence may depend on even broader-scale effects of fire weather, with small-scale variability failing to influence fire behavior under extreme conditions (11, 106), though we did not detect such an interaction between our metric of burning conditions (100-hour fuel moisture) and variability in forest structure.

Correlation between covariates and interactions

Unexpectedly, we found a strong interaction between the prefire NDVI at a pixel and its neighborhood mean NDVI on the probability of high-severity fire. These two variables are strongly correlated (Spearman's $\rho =$ 0.97), so the general effect of this interaction is to dampen the dominating effect of prefire NDVI. Thus, though the marginal effect of prefire NDVI on the probability of high-severity fire is still positive and large, its real-world effect might be more comparable to other modeled covariates when including the negative main effect of neighborhood mean NDVI, the negative interaction effect of prefire NDVI and neighborhood mean NDVI, and their tendency to covary (compare the effect of vegetation density under the common scenario of prefire NDVI and neighborhood mean NDVI increasing or decreasing together: $\beta_{\text{prefire\_ndvi}} + \beta_{\text{nbhd\_mean\_NDVI}} + \beta_{\text{nbhd\_mean\_NDVI*prefire\_NDVI}} = 0.331$, to the effect of 100-hour fuel moisture, which becomes the effect with the greatest magnitude: $\beta_{\text{fm100}} =$ -0.569).

In the few cases when prefire NDVI and the neighborhood mean NDVI contrast, there is an overall effect of increasing the probability of high-severity fire. When prefire NDVI at the central pixel is high and the neighborhood NDVI is low (e.g., an isolated vegetation patch; Supplemental Fig. 2), the probability of high-severity fire is expected to dramatically increase. When prefire NDVI at the central pixel is low and the neighborhood NDVI is high (e.g., a hole in the center of an otherwise dense forest; Supplemental Fig. 2), the probability of high-severity fire at that central pixel is still expected to be fairly high even though there is limited vegetation density (see Supplemental Fig. 2). In these forest NDVI datasets, when these variables do decouple, they tend to do so in the "hole in the forest" case and lead to a greater probability of high-severity fire at the central pixel despite the lower vegetation density there. This can perhaps be explained if the consistently high vegetation density in a local neighborhood– itself more likely to burn at high-severity– exerts a contagious effect on the central pixel, raising its probability of burning at high-severity regardless of how much fuel might be there to burn.

A new approach to remotely sensing wildfire severity

We developed an approach to calculating wildfire severity leveraging the cloud-based data catalog, the large parallel processing system, and the distribution of computation tasks in Google Earth Engine to enable rapid high-throughput analyses of earth observation data (52). Our programmatic assessment of wildfire severity across the 972 Sierra Nevada yellow pine/mixed-conifer fires in the FRAP perimeter database, which enabled consistent assessment of severity for a broad representation of fires including smaller events (60). We found that the relative burn ratio (RBR) calculated using prefire Landsat images collected over a 48-day period prior to the fire and postfire Landsat images collected over a 48-day period one year after the prefire images validated the best with ground-based severity measurements (composite burn index; CBI). Further, we found that this programmatic approach was robust to a wide range of severity metrics, time windows, and interpolation techniques.

We echo the conclusion of (63) that the validation of differences between pre- and postfire NDVI to field-measured severity data, which uses near infrared reflectance, is comparable to validation using more commonly used severity metrics (e.g., RdNBR and RBR) that rely on short wave infrared reflectance. One immediately operational implication of this is that the increasing availability of low-cost small unhumanned aerial systems (sUAS a.k.a. drones) and near-infrared-detecting imagers (e.g., those used for agriculture monitoring) may be used to reliably assess wildfire severity at very high spatial resolutions.

Conclusions

While the severity of a wildfire in any given place is controlled by many variables, we have presented strong evidence that, across large areas of forest, variable forest structure generally makes yellow pine/mixed-conifer forest in the Sierra Nevada more resistant to this inevitable disturbance. It has been well-documented that frequent, low-severity wildfire maintains forest structural variability. Here, we demonstrate a system-wide reciprocal effect suggesting that greater local-scale variability of vegetation structure makes fire-prone, dry forests more resilient to wildfire and may increase the probability of their long-term persistence.

Acknowledgements

We thank Connie Millar, Derek Young, and Meagan Oldfather for valuable comments about this work and we also thank the community of Google Earth Engine developers for prompt and helpful insights about the platform. We thank two anonymous reviewers for their helpful comments on the manuscript. Funding was provided by NSF Graduate Research Fellowship Grant #DGE- 1321845 Amend. 3 (to MJK).

References

1. Hansen MC, et al. (2013) High-Resolution Global Maps of 21st-Century Forest Cover Change. *Science* 342(6160):850–853.

2. Crowther TW, et al. (2015) Mapping tree density at a global scale. *Nature* 525(7568):201–205.

3. Millar CI, Stephenson NL (2015) Temperate forest health in an era of emerging megadisturbance. *Science* 349(6250):823–826.

4. Trumbore S, Brando P, Hartmann H (2015) Forest health and global change. *Science* 349(6250):814–818.

5. Seidl R, Spies TA, Peterson DL, Stephens SL, Hicke JA (2016) Searching for resilience: Addressing the impacts of changing disturbance regimes on forest ecosystem services. *J Appl Ecol* 53(1):120–129.

6. Schoennagel T, et al. (2017) Adapt to more wildfire in western North American forests as climate changes. *Proceedings of the National Academy of Sciences* 114(18):4582–4590.

7. Holling CS (1973) Resilience and Stability of Ecological Systems. *Annual Review of Ecology and Systematics*:1–23.

8. Walker B, Holling CS, Carpenter SR, Kinzig AP (2004) Resilience, Adaptability and Transformability in Social-ecological Systems. *Ecology and Society* 9(2). doi:10.5751/ES-00650-090205.

9. Scheffer M (2009) *Critical Transitions in Nature and Society* (Princeton University Press).

10. Reyer CPO, et al. (2015) Forest resilience and tipping points at different spatio-temporal scales: Approaches and challenges. *Journal of Ecology* 103(1):5–15.

11. Peters DPC, et al. (2004) Cross-scale interactions, nonlinearities, and forecasting catastrophic events.

Proceedings of the National Academy of Sciences 101(42):15130–15135.

12. Reusch TBH, Ehlers A, Hammerli A, Worm B (2005) Ecosystem recovery after climatic extremes enhanced by genotypic diversity. *Proceedings of the National Academy of Sciences* 102(8):2826–2831.

13. Baskett ML, Gaines SD, Nisbet RM (2009) Symbiont diversity may help coral reefs survive moderate climate change. *Ecological Applications* 19(1):3–17.

14. Agashe D (2009) The Stabilizing Effect of Intraspecific Genetic Variation on Population Dynamics in Novel and Ancestral Habitats. *The American Naturalist* 174(2):255–267.

15. Tilman D (1994) Competition and Biodiversity in Spatially Structured Habitats. *Ecology* 75(1):2–16.

16. Chesson P (2000) Mechanisms of Maintenance of Species Diversity. *Annual Review of Ecology and Systematics* 31(1):343–366.

17. Cadotte M, Albert CH, Walker SC (2013) The ecology of differences: Assessing community assembly with trait and evolutionary distances. *Ecology Letters* 16(10):1234–1244.

18. Gazol A, Camarero JJ (2016) Functional diversity enhances silver fir growth resilience to an extreme drought. *Journal of Ecology* 104(4):1063–1075.

19. Ackerly DD, et al. (2010) The geography of climate change: Implications for conservation biogeography: Geography of climate change. *Diversity and Distributions* 16(3):476–487.

20. Lenoir J, et al. (2013) Local temperatures inferred from plant communities suggest strong spatial buffering of climate warming across Northern Europe. *Global Change Biology* 19(5):1470–1481.

21. Questad EJ, Foster BL (2008) Coexistence through spatio-temporal heterogeneity and species sorting in grassland plant communities. *Ecology Letters* 11(7):717–726.

22. Reyer CP, Rammig A, Brouwers N, Langerwisch F (2015) Forest resilience, tipping points and global change processes. *Journal of Ecology* 103(1):1–4.

23. Keeley JE (2009) Fire intensity, fire severity and burn severity: A brief review and suggested usage. *International Journal of Wildland Fire* 18(1):116.

24. Stevens JT, Collins BM, Miller JD, North MP, Stephens SL (2017) Changing spatial patterns of stand-replacing fire in California conifer forests. *Forest Ecology and Management* 406:28–36.

25. Davis KT, et al. (2019) Wildfires and climate change push low-elevation forests across a critical climate

threshold for tree regeneration. *PNAS*:201815107.

26. Safford HD, Stevens JT (2017) *Natural Range of Variation for Yellow Pine and Mixed-Conifer Forests in the Sierra Nevada, Southern Cascades, and Modoc and Inyo National Forests, California, USA*.

27. Welch KR, Safford HD, Young TP (2016) Predicting conifer establishment post wildfire in mixed conifer forests of the North American Mediterranean-climate zone. *Ecosphere* 7(12):e01609.

28. Young DJN, et al. (2019) Post-fire forest regeneration shows limited climate tracking and potential for drought-induced type conversion. *Ecology* 100(2):e02571.

29. Collins BM, Roller GB (2013) Early forest dynamics in stand-replacing fire patches in the northern Sierra Nevada, California, USA. *Landscape Ecology* 28(9):1801–1813.

30. Coppoletta M, Merriam KE, Collins BM (2016) Post-fire vegetation and fuel development influences fire severity patterns in reburns. *Ecological Applications* 26(3):686–699.

31. Williams AP, et al. (2013) Temperature as a potent driver of regional forest drought stress and tree mortality. *Nature Climate Change* 3(3):292–297.

32. Clark JS, et al. (2016) The impacts of increasing drought on forest dynamics, structure, and biodiversity in the United States. *Global Change Biology* 22(7):2329–2352.

33. Fried JS, Torn MS, Mills E (2004) The Impact of Climate Change on Wildfire Severity: A Regional Forecast for Northern California. *Climatic Change* 64(1/2):169–191.

34. Abatzoglou JT, Williams AP (2016) Impact of anthropogenic climate change on wildfire across western US forests. *Proceedings of the National Academy of Sciences* 113(42):11770–11775.

35. Stevens-Rumann CS, et al. (2018) Evidence for declining forest resilience to wildfires under climate change. *Ecology Letters* 21(2):243–252.

36. Miller JD, Thode AE (2007) Quantifying burn severity in a heterogeneous landscape with a relative version of the delta Normalized Burn Ratio (dNBR). *Remote Sensing of Environment* 109(1):66–80.

37. Steel ZL, Koontz MJ, Safford HD (2018) The changing landscape of wildfire: Burn pattern trends and implications for California's yellow pine and mixed conifer forests. *Landscape Ecology* 33(7):1159–1176.

38. Stephens SL, Fry DL, Franco-Vizcaíno E (2008) Wildfire and Spatial Patterns in Forests in Northwestern Mexico: The United States Wishes It Had Similar Fire Problems. *Ecology and Society* 13(2). doi:10.5751/ES-

02380-130210.

39. North M, Stine P, O'Hara K, Zielinski W, Stephens S (2009) *An ecosystem management strategy for Sierran mixed-conifer forests* (U.S. Department of Agriculture, Forest Service, Pacific Southwest Research Station, Albany, CA) doi:10.2737/PSW-GTR-220.

40. Virah-Sawmy M, Gillson L, Willis KJ (2009) How does spatial heterogeneity influence resilience to climatic changes? Ecological dynamics in southeast Madagascar. *Ecological Monographs* 79(4):557–574.

41. Agee JK (1996) The influence of forest structure on fire behavior. *17th Forest Vegetation Management Conference*:17.

42. Scott JH, Reinhardt ED (2001) *Assessing crown fire potential by linking models of surface and crown fire behavior* (U.S. Department of Agriculture, Forest Service, Rocky Mountain Research Station, Ft. Collins, CO) doi:10.2737/RMRS-RP-29.

43. Graham RT, McCaffrey S, Jain TB (2004) *Science basis for changing forest structure to modify wildfire behavior and severity* (U.S. Department of Agriculture, Forest Service, Rocky Mountain Research Station, Ft. Collins, CO) doi:10.2737/RMRS-GTR-120.

44. Stephens SL, et al. (2009) Fire treatment effects on vegetation structure, fuels, and potential fire severity in western U.S. forests. *Ecological Applications* 19(2):305–320.

45. Fox JM, Whitesides GM (2015) Warning signals for eruptive events in spreading fires. *Proceedings of the National Academy of Sciences* 112(8):2378–2383.

46. Sugihara NG, Wagtendonk JWV, Fites-Kaufman J, Shaffer KE, Thode AE (2006) *Fire in California's ecosystems* (University of California Press) Available at: https://nau.pure.elsevier.com/en/publications/fire-in-californias-ecosystems [Accessed April 23, 2019].

47. Scholl AE, Taylor AH (2010) Fire regimes, forest change, and self-organization in an old-growth mixed-conifer forest, Yosemite National Park, USA. *Ecological Applications* 20(2):362–380.

48. Moritz MA, Morais ME, Summerell LA, Carlson JM, Doyle J (2005) Wildfires, complexity, and highly optimized tolerance. *Proceedings of the National Academy of Sciences* 102(50):17912–17917.

49. Graham LJ, Spake R, Gillings S, Watts K, Eigenbrod F (2019) Incorporating fine-scale environmental heterogeneity into broad-extent models. *Methods in Ecology and Evolution* 10(6):767–778.

50. Kotliar NB, Wiens JA (1990) Multiple Scales of Patchiness and Patch Structure: A Hierarchical Framework

for the Study of Heterogeneity. *Oikos* 59(2):253.

51. Turner MG, Donato DC, Romme WH (2013) Consequences of spatial heterogeneity for ecosystem services in changing forest landscapes: Priorities for future research. *Landscape Ecology* 28(6):1081–1097.

52. Gorelick N, et al. (2017) Google Earth Engine: Planetary-scale geospatial analysis for everyone. *Remote Sensing of Environment* 202:18–27.

53. Haralick RM, Shanmugam K, Dinstein I (1973) Textural Features for Image Classification. *IEEE Transactions on Systems, Man, and Cybernetics* SMC-3(6):610–621.

54. JepsonFloraProject ed. (2016) *Jepson eFlora* Available at: http://ucjeps.berkeley.edu/eflora/ [Accessed March 7, 2016].

55. Eidenshink J, et al. (2007) A Project for Monitoring Trends in Burn Severity. *Fire Ecology* 3(1):3–21.

56. Masek J, et al. (2006) A Landsat Surface Reflectance Dataset for North America, 19902000. *IEEE Geoscience and Remote Sensing Letters* 3(1):68–72.

57. Vermote E, Justice C, Claverie M, Franch B (2016) Preliminary analysis of the performance of the Landsat 8/OLI land surface reflectance product. *Remote Sensing of Environment* 185:46–56.

58. USGS (2017) Landsat 8 Surface Reflectance Code (LASRC) Product Guide. 40.

59. USGS (2017) Landsat 4-7 Surface Reflectance (LEDAPS) Product Guide. 41.

60. Randerson JT, Chen Y, Werf GR van der, Rogers BM, Morton DC (2012) Global burned area and biomass burning emissions from small fires. *Journal of Geophysical Research: Biogeosciences* 117(G4). doi:10.1029/2012JG002128.

61. Miller JD, Skinner CN, Safford HD, Knapp EE, Ramirez CM (2012) Trends and causes of severity, size, and number of fires in northwestern California, USA. *Ecological Applications* 22(1):184–203.

62. Miller JD, Safford H (2012) TRENDS IN WILDFIRE SEVERITY: 1984 TO2010 IN THE SIERRA NEVADA, MODOC PLATEAU, AND SOUTHERN CASCADES, CALIFORNIA, USA. *Fire Ecology* 8(3):41–57.

63. Zhu Z, Key C, Ohlen D, Benson N (2006) *Evaluate Sensitivities of Burn-Severity Mapping Algorithms for Different Ecosystems and Fire Histories in the United States.*

64. Sikkink PG, et al. (2013) Composite Burn Index (CBI) data and field photos collected for the FIRESEV

project, western United States. doi:10.2737/RDS-2013-0017.

65. Key CH, Benson NC (2006) Landscape Assessment (LA). 55.

66. Miller JD, et al. (2009) Calibration and validation of the relative differenced Normalized Burn Ratio (RdNBR) to three measures of fire severity in the Sierra Nevada and Klamath Mountains, California, USA. *Remote Sensing of Environment* 113(3):645–656.

67. Cansler CA, McKenzie D (2012) How Robust Are Burn Severity Indices When Applied in a New Region? Evaluation of Alternate Field-Based and Remote-Sensing Methods. *Remote Sensing* 4(2):456–483.

68. Parks S, Dillon G, Miller C (2014) A New Metric for Quantifying Burn Severity: The Relativized Burn Ratio. *Remote Sensing* 6(3):1827–1844.

69. Prichard SJ, Kennedy MC (2014) Fuel treatments and landform modify landscape patterns of burn severity in an extreme fire event. *Ecological Applications* 24(3):571–590.

70. Parks SA, et al. (2018) High-severity fire: Evaluating its key drivers and mapping its probability across western US forests. *Environmental Research Letters* 13(4):044037.

71. Wickham H (2019) *Modelr: Modelling Functions that Work with the Pipe* Available at: https://CRAN.R-project.org/package=modelr.

72. Henry L, Wickham H (2019) *Purrr: Functional Programming Tools* Available at: https://CRAN.R-project.org/package=purrr.

73. R Core Team (2018) *R: A language and environment for statistical computing* (R Foundation for Statistical Computing, Vienna, Austria) Available at: https://www.R-project.org/.

74. Tuanmu M-N, Jetz W (2015) A global, remote sensing-based characterization of terrestrial habitat heterogeneity for biodiversity and ecosystem modelling: Global habitat heterogeneity. *Global Ecology and Biogeography* 24(11):1329–1339.

75. Rouse W, Haas RH, Deering W, Schell JA (1973) *Monitoring the vernal advancement and retrogradation (green wave effect) of natural vegetation* (Goddard Space Flight Center, Greenbelt, MD, USA).

76. Franklin J, Logan T, Woodcock C, Strahler A (1986) Coniferous Forest Classification and Inventory Using Landsat and Digital Terrain Data. *IEEE Transactions on Geoscience and Remote Sensing* GE-24(1):139–149.

77. Lydersen JM, Collins BM, Knapp EE, Roller GB, Stephens S (2015) Relating fuel loads to overstorey structure and composition in a fire-excluded Sierra Nevada mixed conifer forest. *International Journal of*

Wildland Fire 24(4):484.

78. Collins BM, et al. (2016) Variability in vegetation and surface fuels across mixed-conifer-dominated landscapes with over 40 years of natural fire. *Forest Ecology and Management* 381:74–83.

79. Stephens SL, et al. (2012) The Effects of Forest Fuel-Reduction Treatments in the United States. *BioScience* 62(6):549–560.

80. Farr TG, et al. (2007) The Shuttle Radar Topography Mission. *Reviews of Geophysics* 45(2). doi:10.1029/2005RG000183.

81. McCune B, Keon D (2002) Equations for potential annual direct incident radiation and heat load. *Journal of Vegetation Science* 13(4):603–606.

82. McCune B (2007) Improved estimates of incident radiation and heat load using non- parametric regression against topographic variables. *Journal of Vegetation Science* 18(5):751–754.

83. Abatzoglou JT (2013) Development of gridded surface meteorological data for ecological applications and modelling. *International Journal of Climatology* 33(1):121–131.

84. Vehtari A, Gelman A, Gabry J (2017) Practical Bayesian model evaluation using leave-one-out cross-validation and WAIC. *Statistics and Computing* 27(5):1413–1432.

85. Hoffman MD, Gelman A (2014) The No-U-Turn Sampler: Adaptively Setting Path Lengths in Hamiltonian Monte Carlo. *Journal of Machine Learning Research* 15:31.

86. Bürkner P-C (2017) **brms**: An *R* package for bayesian multilevel models using *Stan*. *Journal of Statistical Software* 80(1). doi:10.18637/jss.v080.i01.

87. Edwards AC, Russell-Smith J, Maier SW (2018) A comparison and validation of satellite-derived fire severity mapping techniques in fire prone north Australian savannas: Extreme fires and tree stem mortality. *Remote Sensing of Environment* 206:287–299.

88. Gelman A, Goodrich B, Gabry J, Vehtari A (2018) R-squared for Bayesian regression models. *The American Statistician*:1–6.

89. Heffernan JB, et al. (2014) Macrosystems ecology: Understanding ecological patterns and processes at continental scales. *Frontiers in Ecology and the Environment* 12(1):5–14.

90. Beck J, et al. (2012) What's on the horizon for macroecology? *Ecography* 35(8):673–683.

91. Folke C, et al. (2004) Regime Shifts, Resilience, and Biodiversity in Ecosystem Management. *Annual*

Review of Ecology, Evolution, and Systematics 3:557–581.

92. Keith DA, et al. (2013) Scientific Foundations for an IUCN Red List of Ecosystems. *PLoS ONE* 8(5):e62111.

93. Turner MG, Romme WH, Gardner RH, Hargrove WW (1997) Effects of Fire Size and Pattern on Early Succession in Yellowstone National Park. *Ecological Monographs* 67(4):411.

94. Holden ZA, Morgan P, Evans JS (2009) A predictive model of burn severity based on 20-year satellite-inferred burn severity data in a large southwestern US wilderness area. *Forest Ecology and Management* 258(11):2399–2406.

95. Dillon GK, et al. (2011) Both topography and climate affected forest and woodland burn severity in two regions of the western US, 1984 to 2006. *Ecosphere* 2(12):art130.

96. Wagner CEV (1977) Conditions for the start and spread of crown fire. *Can J For Res* 7(1):23–34.

97. Agee JK, Skinner CN (2005) Basic principles of forest fuel reduction treatments. *Forest Ecology and Management* 211(1-2):83–96.

98. Rose KC, et al. (2017) Historical foundations and future directions in macrosystems ecology. *Ecology Letters* 20(2):147–157.

99. Larson AJ, Churchill D (2012) Tree spatial patterns in fire-frequent forests of western North America, including mechanisms of pattern formation and implications for designing fuel reduction and restoration treatments. *Forest Ecology and Management* 267:74–92.

100. Malone S, et al. (2018) Mixed-Severity Fire Fosters Heterogeneous Spatial Patterns of Conifer Regeneration in a Dry Conifer Forest. *Forests* 9(1):45.

101. Walker RB, Coop JD, Parks SA, Trader L (2018) Fire regimes approaching historic norms reduce wildfire-facilitated conversion from forest to non-forest. *Ecosphere* 9(4):e02182.

102. Wagtendonk JWV (2006) *Fire as a Physical Process* (University of California Press) Available at: http://california.universitypressscholarship.com/view/10.1525/california/9780520246058.001.0001/upso-9780520246058-chapter-3 [Accessed April 23, 2019].

103. Miller JD, Safford HD (2017) Corroborating Evidence of a Pre-Euro-American Low- to Moderate-Severity Fire Regime in Yellow PineMixed Conifer Forests of the Sierra Nevada, California, USA. *Fire Ecology* 13(1):58–90.

104. Safford H, Stevens J, Merriam K, Meyer M, Latimer A (2012) Fuel treatment effectiveness in California

yellow pine and mixed conifer forests. *Forest Ecology and Management* 274:17–28.

105. Tubbesing CL, et al. (2019) Strategically placed landscape fuel treatments decrease fire severity and promote recovery in the northern Sierra Nevada. *Forest Ecology and Management* 436:45–55.

106. Lydersen JM, North MP, Collins BM (2014) Severity of an uncharacteristically large wildfire, the Rim Fire, in forests with relatively restored frequent fire regimes. *Forest Ecology and Management* 328:326–334.